An Analytical Determination of Speed Factor in Gear Designs

Dynamic photoelasticity, fatigue testing and cumulative-damage concept enable an analytical determination of speed factor formerly expressed in empirical forms

by S. Shimamura and Y. Noguchi

ABSTRACT—In practical gear design, the "speed factor" is usually employed which is defined as a ratio of the allowable stress at required running speed of the gear system to the stress at zero speed. At present, several expressions for the speed factor are recommended by several authorities; however, those are almost all empirical and not analytical.

The present paper aims to contribute to an analytical determination of the speed factor for spur gears as stated below.

First, from a dynamic photoelastic test of a pair of spur gears, the following results were obtained:

(1) At a constant speed and torque and at the same point of engagement, the maximum fillet stress did not have a specific constant value but had somewhat scattered values due to the vibration of gear system under operation.

(2) The mean value of the scattered stresses was almost constant and less dependent on the running speed of gears; however, the range of scatter, i.e., the standard deviation, was significantly dependent on the speed and rapidly increased with an increase in the speed.

Next, flexural fatigue testing was conducted with the epoxy resin, the photoelastic material, and the S–N diagram was determined.

Finally, the cumulative-damage concept was applied into the fatigue failure of the gear tooth where the above-determined hystogram of fillet stresses and the S–N diagram were used; then, the allowable mean stress which ensures 10^7 endurance was estimated for each running speed. An analytical value of the speed factor was then determined by dividing the allowable stress by the fatigue strength of the material at 10^7 cycles. The speed factor thus obtained was compared with the conventional expressions for the speed factor.

S. Shimamura and Y. Noguchi are Senior Research Officer and Research Officer, respectively, Government Mechanical Laboratory, Tokyo, Japan.

Paper was presented by title at Second SESA International Congress on Experimental Mechanics held in Washington, D. C., on Sept. 28–Oct. 1, 1965.

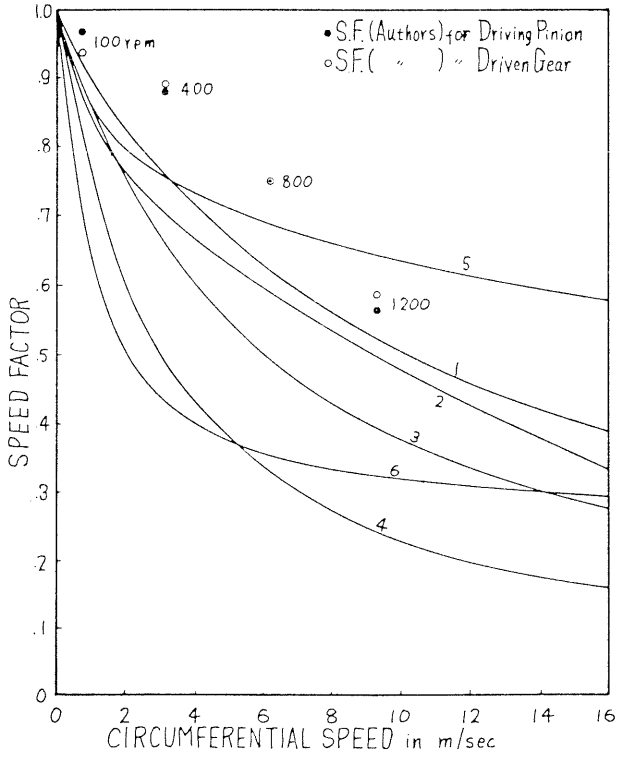

Fig. 1—Speed factor vs. circumferential speed. Authors' result is compared with conventional expressions for the speed factor. Curves represent following expressions, respectively (v = circumferential speed in m/sec or f/min):

1. Speed factor = 10/(10+v) (v:m/sec) (after Rötscher)
2. Speed factor = $1-(\sqrt{v}/84)$ (v:f/min) (after AGMA)
3. Speed factor = 1200/(1200+v) (v:f/min) (after Birth)
4. Speed factor = 600/(600+v) (v:f/min) (after Birth)
5. Speed factor = $78/(78+\sqrt{v})$ (v:f/min) (after Rusmussen)
6. Speed factor = $\{150/(200+v)\}+0.25$ (v:f/min) (after AGMA for nonmetallic gear)

List of Symbols

N = number of cycles to failure
N_i = number of cycles to failure under constant amplitude of alternating stress, S_i
N_t = number of cycles to failure under varying amplitude of alternating stress
n_i = number of cycles of stress, S_i
n_0 = sum of n_i
S = alternating stress or maximum fillet stress
$\bar{S}$ = mean of S
σ = standard deviation of S

Introduction

The speed factor, as defined in eq (1), is usually adopted in gear-design practice to ensure the life of gear system under operation:

$$\text{speed factor} = \frac{\text{allowable stress at required running speed}}{\text{allowable stress at zero speed}} \quad (1)$$

Now, several expressions for the speed factor are recommended by several authorities as shown in Fig. 1; however, these are mostly empirical and not analytical.

From the viewpoint of the fatigue strength, the

speed factor is a safety factor ensuring the same endurance life of gears for various running speeds. Then the speed factor shall be determined from the following three points.

(1) Since it is the usual practice to express a life of a gear as a period, i.e., hours or years, and not cycles to failure, an increase in running speed results in an increase in number of stress cycles per unit time; so, for a certain predetermined life expressed in years, more stress cycles must be endured to failure. In this connection, it is clear that the greater the speed the less the allowable stress, namely, the lower the speed factor to be employed; this is easily evaluated from the S–N diagram of the gear material. In the scope of the present paper this factor is not included.

(2) If the mean of the tensile fillet stresses (or the maximum shearing stresses in the vicinity of the point of engagement) increases with the increase in the running speed, the allowable design stress shall be reduced to ensure same life (in cycles), and this is also easily determined from S–N diagram. As clarified below, the mean of dynamic stresses was less dependent on the speed in the present test condition, and therefore this factor was not considered.

(3) Finally, the most interesting is an effect of the scatter of dynamic stresses, that is, how the value of $\bar{S}$ shall be selected to ensure the same life for different running speeds when the relative degree of scatter in dynamic stresses, i.e., coefficients of variation, is known. The aim of the present paper is focused on this point.

The present paper aims to contribute to an analytical determination of the speed factor and is composed of three parts such as dynamic photoelasticity, fatigue testing and application of the cumulative damage concept.

Dynamic Photoelasticity in Spur Gears

An application of the dynamical photoelastic technique in the stress analysis of operating gears is not new. From the Coker's age, several photoelasticians have tried to determine the dynamic stresses in gears photoelastically[1–10]; however, from the authors' viewpoint, those were mostly trials and no contributions were made to an analytical determination of the speed factor. The reason why the former work in this branch has failed to clarify the nature of dynamic stresses in gears is, very likely, as follows: lack of a suitable photoelastic material, high-sensitivity photographic material and high-intensity stroboscopic light source. At present, with those materials and devices of much higher quality, it is more feasible to apply the photoelastic technique to dynamic-stress problems in gears.

Model Gear

The driving pinion and the driven gear were of the same design, tooth profile of the standard involute of pressure angle 20 deg, 4 module, pitch diameter 148 mm, 37 teeth. A circular blank turned from epoxy-resin plate 5.6-mm thick was carefully machined by the Pfautor gear-hobbing machine. The completed model was annealed in an electrical furnace according to the usually employed temperature cycle before testing. The fringe value of the epoxy material was 1.05 kg/mm/fringe.

Test Setup

The test setup used is roughly illustrated in Fig. 2. The driving pinion g_1 is driven by a d-c motor M, and the driven gear g_2 is connected with a electrical dynamometer D. By elaborate control of the motor and dynamometer, the required torque within

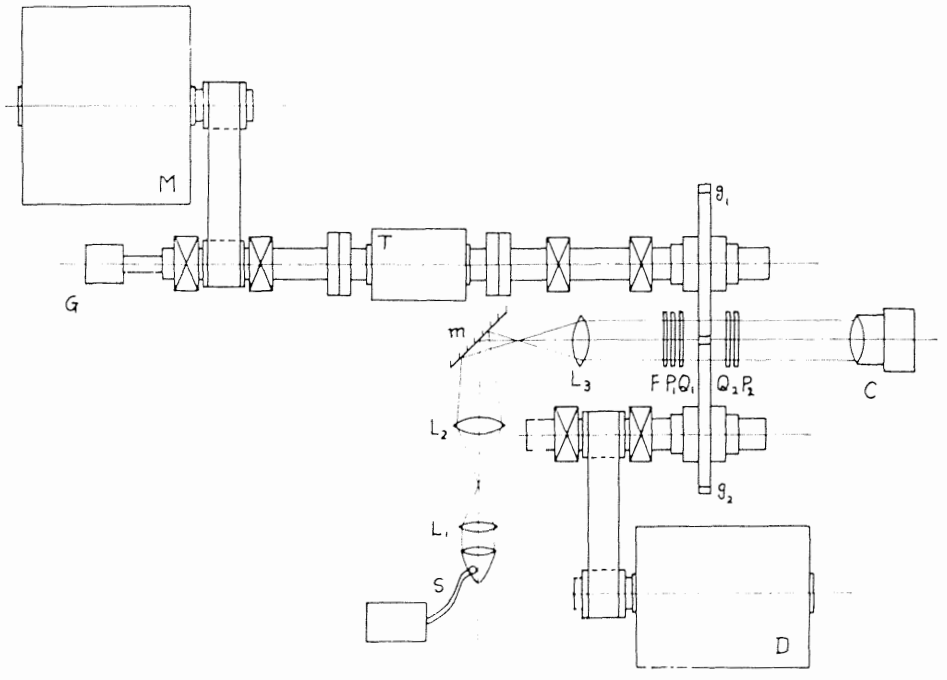

Fig. 2—Test setup (C = camera, D = dynamometer; F = filter; G = tachogenerator; g_1 and g_2 = driving pinion and driven gear; L_1, L_2 and L_3 = lenses; M = d- motor; m = mirror; P_1 and P_2 = polarizer and analyzer; Q_1 and Q_2 = quarter-wave plates; S = strobolume; T = torquemeter)

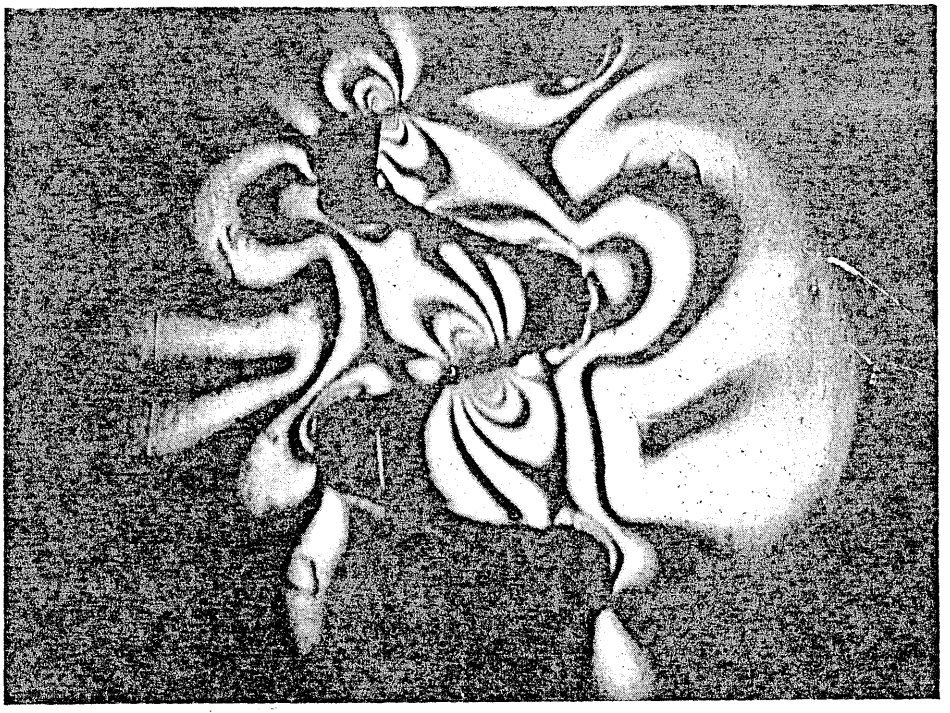

(a)

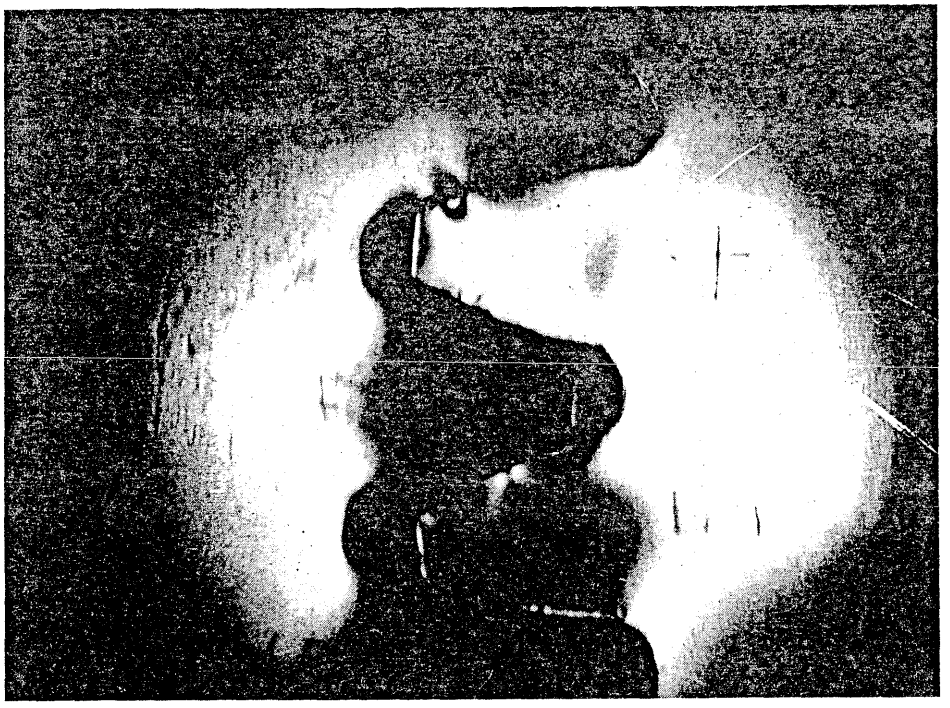

(b)

Fig. 3—Fringe patterns, driving pinion at 1200 rpm. (b) shows idling condition that may occur under operation

0 to 2 kg-m can be applied to the gear system at required revolution speed within 0 to 1200 rpm. Applied torque and revolution speed are measured by a strain-gage torquemeter T and an electrical tachogenerator G, respectively. The distance between the driving and driven shafts may be changed if necessary, according to the size of gears to be tested. The arrangement of optical bench is similar to the ordinary photoelastic apparatus, except that the light pass is turned by 90 deg by a mirror m due to the space limitation in the setup.

Photographing Fringe Patterns

The dynamic-fringe pattern was photographed by using the stroboscopic-light source, Strobolume (General Radio Co.) with a monochromatic filter (green). However, Strobolume was not used for the stroboscopic purpose but used as the instantaneous one-shot light source. At constant speed and torque, about fifty patterns were taken at nearly constant point of engagement (in the vicinity of the pitch diameter). A copying film was used, and an intensified developing technique was applied. The result of photographing was satisfactory. The photoelastic tests were carried out at 100, 400, 800 and 1200 rpm, respectively.

Results

FRINGE PATTERNS—As an interesting example of fringe patterns thus obtained, two patterns are shown in Fig. 3, both are at 1200 rpm and the same torque reading; nevertheless, in Fig. 3(b) an idling

condition (no contact between the pinion and gear) is observed. This probably results from an intermittent and irregular contact (not continuous and smooth transmission of load) between the teeth of driving pinion and driven gear due to the vibration of the gear system. This consideration is firmly supported by Fig. 5, where the scatter of stress values is increased with the increase of speed of gears.

NATURE OF DYNAMIC STRESSES—As shown in Fig. 4, a hystogram of maximum tensile fillet stress of the driving pinion indicates that at 800 rpm, for example, the stress does not have a specific constant value but has somewhat scattered values at a constant speed and torque and at a same point of engagement. The summarized results are expressed in Table 1 and Fig. 5 as the mean value and the standard deviation of the stresses vs. the running speed, where the stress is expressed in fringe order divided by applied torque.

From Fig. 5 and Table 1, it can be concluded that, in the test condition described above, the mean of scattered stress values is almost independent of the running speed of gears, but the scatter, i.e., the standard deviation, is significantly dependent on the speed, and it rapidly increases with an increase in the speed. These are explained as follows: the mean (or median) stress is similar to those statically determined from the applied torque and, therefore, it is little dependent on the speed; to the contrary, the degree of scatter of the stress, i.e., range of the stress hystogram, as shown in Fig. 4, is due to a percussive contact of the teeth and is thus highly dependent on the running speed of the gear system.

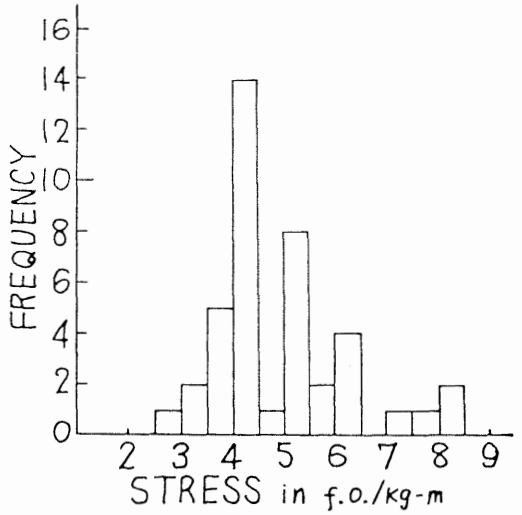

Fig. 4—Hystogram of dynamic stresses for driving pinion at 800 rpm (maximum tensile fillet stress)

Fatigue Testing of Epoxy Resin

In order to apply the cumulative-damage concept as stated in the next section, the determination of the fatigue strength of the epoxy-resin photoelastic material was necessary. In this connection, flexural fatigue testing was carried out with the Baldwin-Sonntag universal fatigue tester. The result was plotted in a S–N diagram as shown in Fig. 6. From this, it was determined that the fatigue strength of the resin at 10^7 cycles was about 1.6 kg/mm².

Determination of Speed Factor

The cumulative-damage concept of Miner[11] states that a fatigue failure under varying stress

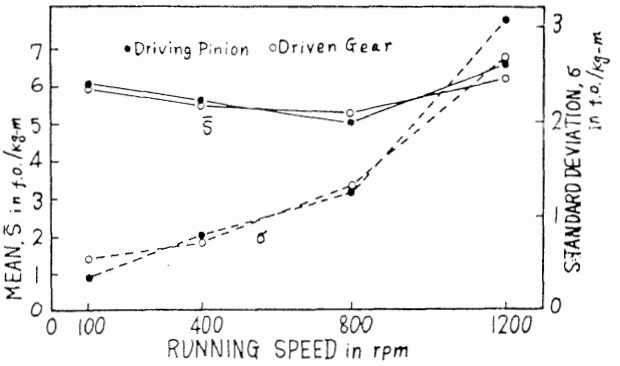

Fig. 5—Mean and standard deviation of dynamic stresses vs. revolution speed (maximum tensile fillet stress)

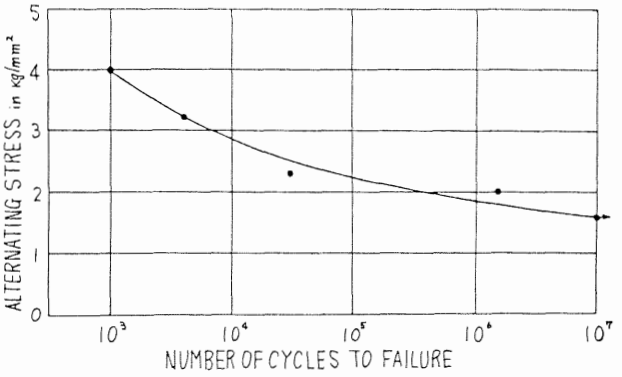

Fig. 6—S–N diagram for epoxy-resin photoelastic material

TABLE 1—MEAN AND STANDARD DEVIATION OF MAXIMUM TENSILE FILLET
(Stress in Fringe Order per kg-m)

rpm	100		400		800		1200	
P & G*	P	G	P	G	P	G	P	G
$\bar{S}$	5.99	5.93	5.55	5.44	4.99	5.26	6.55	6.13
σ	0.38	0.56	0.79	0.74	1.26	1.31	3.08	2.68
$\sigma/\bar{S}$	0.0635	0.0943	0.142	0.136	0.252	0.249	0.471	0.437

* P = driving pinion, G = driven gear.

amplitude occurs when the following condition is satisfied:

$$\sum \frac{n_i}{N_i} = 1 \qquad (2)$$

From eq (2), the following equation is deduced:

$$N_t = n_0 / \Sigma(n_i/N_i) \qquad (3)$$

Now, by assuming the shape of the hystogram of the dynamic stress in gears is of the normal distribution with coefficient of variation $\sigma/\bar{S}$ as tabulated in Table 1, respective values of n_i can be easily determined by using a statistical table. Since N_i is obtained from the S–N diagram in Fig. 6, N_t for varying stress amplitude with $\bar{S}$ and $\sigma/\bar{S}$ can be determined. If the understressing may be neglected, the stress more than 1.6 kg/mm² shall be considered.

In Table 2 is shown an example of such calculation when the revolution speed is 800 rpm, where the range of varying stresses is taken as $\bar{S} + 3\sigma$ and the interval of stress, 0.2 kg/mm². For driving pinion at 800 rpm, N_t* (including cycles of harmless stresses less than 1.6 kg/mm²) are 282×10^4, 1011×10^4 and 3990×10^4 for $\bar{S} = 1.3$, 1.2 and 1.1 kg/mm², respectively. Plotting these values against $\bar{S}$ as shown in Fig. 7, the value of $\bar{S}$ which ensures $N_t^* = 10^7$ can be determined.

Consequently, the speed factor in connection

TABLE 2—NUMERICAL PROCEDURE TO DETERMINE N_t* FOR DRIVING PINION AT 800 RPM

S	p	Δp	n_i	N_i	n_i/N_i	$\sum n_i/N_i$	N_t	N_t*
($\bar{S} = 1.3$,	$\sigma/\bar{S} = 0.252$,	$\sigma = 0.327$)						
1.3	50.0	...	...	...	...	...	...	...
1.4	62.2	...	...	...	...	...	...	...
1.5	72.9	...	...	...	...	...	...	...
1.6	82.1	16.0	160	10^7	0.16×10^{-4}	...	...	...
1.7	88.9	...	...	...	...	...	...	...
1.8	93.7	7.7	77	1.4×10^6	0.55×10^{-4}	...	...	...
1.9	96.6	...	...	...	...	3.54×10^{-4}	76.6×10^4	282×10^4
2.0	98.4	2.7	27	2×10^5	1.35×10^{-4}	...	...	...
2.1	99.3	...	...	...	...	...	...	...
2.2	99.7	0.6	6	6.5×10^4	0.92×10^{-4}	...	...	...
2.3	99.9	...	...	...	...	...	...	...
2.4	99.96	0.1	1	1.8×10^4	0.56×10^{-4}	...	...	...
		$n_0 = 271$						
($\bar{S} = 1.2$,	$\sigma = 0.302$)							
1.2	50.0	...	...	...	...	...	...	...
1.3	62.9	...	...	...	...	...	...	...
1.4	74.5	...	...	...	...	...	...	...
1.5	83.9	...	...	...	...	...	...	...
1.6	90.7	11.3	113	10^7	0.113×10^{-4}	...	...	...
1.7	95.2	...	...	...	...	...	...	...
1.8	97.7	3.8	38	1.4×10^6	0.272×10^{-4}	...	...	...
1.9	99.0	...	...	...	...	0.989×10^{-4}	163×10^4	1011×10^4
2.0	99.6	0.9	9	2×10^5	0.45×10^{-4}			
2.1	99.9	...	...	...	...	...	...	...
2.2	99.95	0.1	1	6.5×10^4	0.154×10^{-4}	...	...	...
		$n_0 = 161$						
($\bar{S} = 1.1$,	$\sigma = 0.276$)							
1.1	50.0	...	...	...	...	...	...	...
1.2	64.1	...	...	...	...	...	...	...
1.3	76.4	...	...	...	...	...	...	...
1.4	86.2	...	...	...	...	...	...	...
1.5	92.7	...	...	...	...	...	...	...
1.6	96.5	5.8	58	10^7	0.058×10^{-4}	...	...	...
1.7	98.5	...	...	...	...	...	...	...
1.8	99.5	1.3	13	1.4×10^6	0.093×10^{-4}	0.251×10^{-4}	291×10^4	3990×10^4
1.9	99.8	...	...	...	...	...	...	...
2.0	99.9	0.19	2	2×10^5	0.10×10^{-4}	...	...	...
2.1	99.99	...	...	...	...	...	...	...
		$n_0 = 73$						

Note: p = cumulative frequency in %.
Δp = difference in p between two adjacent values of S.
N_t* = total number of cycles to failure under the stress with given hystogram and equals to N_t multiplied by ($1000/n_0$).

TABLE 3—MEAN STRESS, $\bar{S}$, WHICH ENSURES $N_t^* = 10^7$ AND SPEED FACTOR FOR DIFFERENT RUNNING SPEEDS

rpm	100		400		800		1200	
P & G,	P	G	P	G	P	G	P	G
$\bar{S}$	1.542	1.494	1.404	1.418	1.201	1.203	0.905	0.939
Speed factor (= S/1.6)	0.964	0.934	0.878	0.887	0.751	0.752	0.566	0.587

Note: P = driving pinion, G = driven gear.

with the scatter of dynamic stresses as described in paragraph (3) of "Introduction" is determined as a ratio between $\bar{S}$ for $N_t^* = 10^7$ already obtained and $\bar{S}$ when the scatter is zero, namely equals to 1.6 kg/mm². In Table 3, speed factors thus evaluated are tabulated. These are also plotted in Fig. 1 in comparison with the conventional expressions for the speed factor.

Examining Fig. 1, it can be concluded that the speed factor thus obtained is qualitatively in good agreement with conventional factors, the discrepancy observed between the authors' data and conventional empirically deduced ones can be explained that the former concerns only the effect of the scatter of dynamic stresses on the fatigue strength of gears and disregards the effect of factors in paragraphs (1) and (2) of the "Introduction."

Conclusion

Application of dynamic photoelasticity to the analysis of stresses in spur gears under operation showed that, under the test condition specified above, the higher the running speed the wider the scatter of dynamic stresses; i.e., the standard deviation increased with the increase in the speed. However, the mean of dynamic stresses was less dependent on the speed.

Next, the flexural fatigue testing of the photoelastic material was carried out and the S–N diagram was constructed.

Finally, the cumulative-damage concept was applied to determine the effect of repeated stress with varying amplitude on the fatigue strength of the gear tooth and the speed factor was determined.

The speed factor analytically determined in such a manner can well explain the characteristics of conventional expressions for the speed factor which were mostly deduced from experience or the result of running tests. Quantitative difference between both factors can be explained as caused by additional effect of other factors neglected in the present paper.

In conclusion, though the present paper is only a particular result for the speed factor for casting epoxy gears, the authors' procedure can be used as a basis in analytical determination of the speed factor for steel gears. In this case of steel gears, the photoelastic-coating technique may be satisfactory. The present investigation concerned only the flexural stress and strength of gear teeth and not the rolling-contact fatigue which occurred at the flank of gear tooth, which is more important than the flexural fatigue in the practical gear-design practice. However, authors' subsequent analysis on

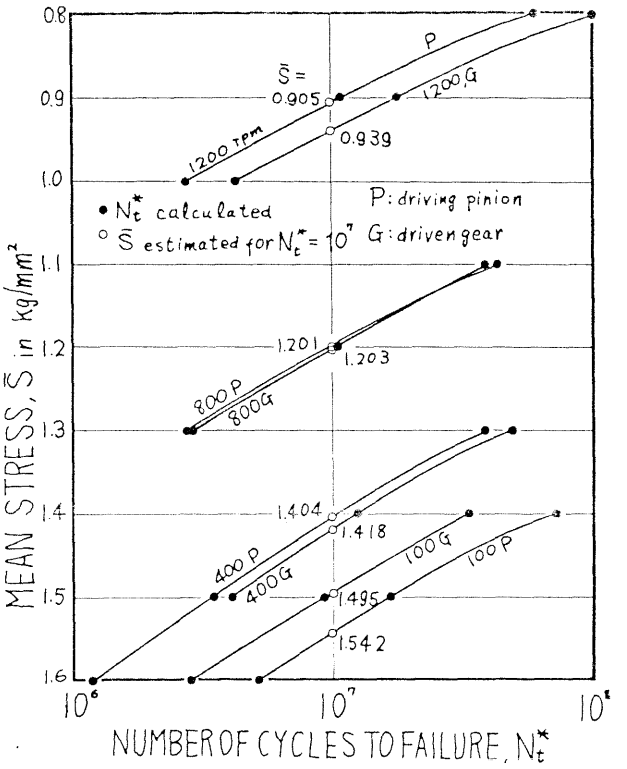

Fig. 7—Procedure to determine $\bar{S}$ for 10^7 endurance for different revolution speed

the behavior of the maximum shearing stress in the vicinity of the point of engagement produced a similar result as in the maximum tensile fillet stress (scatter of stress is significant and the mean of stress is less dependent on the speed). Therefore, if S–N diagram for the epoxy resin under rolling-contact fatigue is obtained, the speed factor for this condition may be easily determined as well.

Acknowledgment

Authors wish to express their thanks to Miss H. Kosaka, M. Yamaki and M. Suzuki for valuable assistance in the experimental work and the numerical calculation.

References

1. *Kimball, A. L., G. E. Rev.*, **27**, *130 (1924).*
2. *Heymans, P., and Kimball, A. L., Mech. Engrg.*, **46**, *129 (1924).*
3. *Kimball, A. L., Am. Mach.*, **63**, *51 (1925).*
4. *Timoshenko, S., and Baud, R. V., Mech. Engrg.*, **48**, *1105 (1926).*
5. *Bradford, H. L., Am. Mach.*, **70**, *393 (1929).*
6. *Am. Mach.*, **71**, *288 (1929).*
7. *Blackman, H. N., Mach. (A)*, **37**, *737 (1931).*
8. *Heywood, R. B., "Tensile Fillet Stresses in Loaded Projections," Proc. IME*, **59**, *391 (1948).*
9. *Tobe, T., "Dynamic Photoelasticity in Spur Gears," Machinery (in Japanese)*, **21**, *1471 (1958).*
10. *Harris, S. L., "Dynamic Loads on the Teeth of Spur Gears," Proc. IME*, **172**, *87 (1958).*
11. *Miner, M. A., "Cumulative Damage in Fatigue," Jnl. Appl. Mech.*, **12**, *159 (1945).*